

Immunoassay on Free-Standing Electrospun Membranes

Dapeng Wu, Daewoo Han, and Andrew J. Steckl*

Nanoelectronics Laboratory, University of Cincinnati, Cincinnati, Ohio 45221-0030

ABSTRACT For the purpose of immunoassay, electrospun membranes can be thought as the threadlike self-assembling of nano/microbeads. Nonwoven membranes of electrospun poly(ϵ -caprolactone) (PCL) fibers display excellent tenacity, flexibility and suitable surface energy. These PCL membranes exhibit easy handling in air, fast spreading, and wetting in aqueous solution, and rapid adsorption of protein molecules by hydrophobic interaction. After a fold-and-press process, the membrane porosity was reduced from $\sim 75\%$ to less than 10% , whereas the thickness increased from 5.3 to $280\ \mu\text{m}$. The resulting fluorescence signal from adsorbed protein increased $> 120\times$. With anti-HSA and HSA-FITC as an immunoassay model, a linear detection range from $500\ \text{ng/mL}$ down to $1\ \text{ng/mL}$ is obtained, with a detection of limit (LOD) of $\sim 0.08\ \text{ng/mL}$. By comparison, conventional nitrocellulose and a $24.3\ \mu\text{m}$ PCL fiber electrospun membrane displayed a much higher LOD of $\sim 100\ \text{ng/mL}$. Immunoassay on free-standing electrospun membrane successfully combines the low-cost and simplicity of conventional membrane immunoassay, with the fast reaction speed and high sensitivity characteristic of magnetic nano/microbeads bioassays.

KEYWORDS: electrospun • free-standing • thin membrane • immunoassay • fold-and-press

INTRODUCTION

Immunoassay is the dominant method to probe target protein in biofluids using the selective recognition and strong binding between antibody and antigen. Heterogeneous immunoassay is the most widely used format based on various solid substrates. Nitrocellulose (NC), poly(vinylidene fluoride) (PVDF), and other conventional, commercial membranes have been widely used as bioassay substrates for DNA (Southern blotting) (1), protein (Western blotting) (2), lateral flow immunochromatographic assays, and common immunoassays (3). After ~ 30 years of usage and development, these membranes have been thoroughly optimized for easy, direct application, and without need for special instrumentation. Membranes of large thickness ($\sim 150\ \mu\text{m}$) are designed for high binding capacity ($\sim 100\ \mu\text{g}/\text{cm}^2$) and free-standing application. However, a consequence of this large volume is that the duration of certain steps (such as antibody immobilization, surface blocking, nonspecific rinsing), is significantly extended ($>4\ \text{h}$). Furthermore, analyte residues are inevitable, leading to high background signal and limited analysis sensitivity (4).

Magnetic beads have been used as new immunoassay substrates in recent years (5, 6). With their small individual size and complete dispersion, the overall large surface area resulted in immuno-reactions that can be completed faster ($<30\ \text{min}$) than using conventional membrane-based techniques. Magnetic bead immunoassays can achieve a very high sensitivity of approximately picomolar to approximately attomolar using signal amplification methods, such as immune-PCR (7), biobarcode assay (BCA) (6), or surface-

enhanced Raman scattering (SERS) (8). However, special tools and/or process steps are required to obtain these high signal gains, such as PCR equipment, controllable nanoparticle fabrication, and special surface functionalization.

In this paper, we report an approach for achieving direct, fast and sensitive immunoassay on thin electrospun membranes. Electrospinning is an efficient and simple tool to spray micro/nano polymer fibers from viscous polymer solutions or melting polymers (9). Nonwoven membranes formed by the aggregation of electrospun fibers have been successfully investigated as scaffolds for cell and tissue culture taking advantage of their large surface area, tunable surface properties, and biodegradability (10). By electrospinning from mixtures of polymers and selected precursors, electrospun fibers have also been widely studied as inorganic nanomaterial carriers for effective dispersion. These inorganic nanoparticle membranes have shown excellent magnetic, optical, and electrical characteristics (9). Coaxial electrospinning of polycaprolactone/Teflon core–sheath fibers has resulted in superhydrophobic membranes (11). Electrospun PVDF and PAN (poly(acrylonitrile)) membranes were also reported (12) to form good matrices for electrodes in fuel cells.

Electrospun membranes have also been tested as sensor and immunoassay substrates. Electrospun fibers with fluorescent indicators have been reported for metal ions (Fe^{3+} or Hg^{2+}) and 2, 4-dinitrotoluene detection (13). PANI (polyaniline)/PEO (polyethylene oxide) nanofibers have been used directly as NH_3 sensors (14). Electrospun polycarbonate (PC) membranes used as immunoassay substrates in microfluidic devices demonstrated (15) $10\times$ stronger signal than that from nanoporous PC films, which is widely utilized for molecule filtration and concentration (16). Electrospun NC and nylon membranes were also used for protein blotting (17). Carboxyl and amine functionalized poly(vinyl chloride)

* To whom correspondence should be addressed. E-mail: a.steckl@uc.edu.

Received for review October 2, 2009 and accepted November 27, 2009

DOI: 10.1021/am900664v

© 2010 American Chemical Society

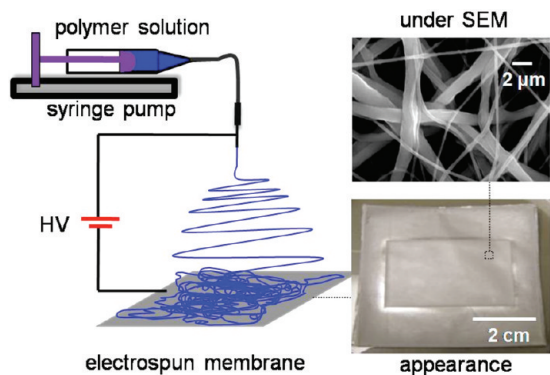


FIGURE 1. Schematic of the electrospinning process. A single syringe pump is used for single polymer solution electrospinning, a dual pump system is used for coaxial electrospinning.

electrospun membranes were used for covalent antibody immobilization (18), and ELISA bioassay of staphylococcal enterotoxin B (SEB) of 1–100 ng/mL using chemiluminescence detection.

In this work, very thin (5.3 μm) electrospun PCL membranes have been used as immunoassay substrates. The membrane can be manipulated freely in air and it spreads out easily in solution. Proteins can adsorb on the electrospun membrane directly from phosphate solution. Similar to the threadlike continuous assembling of nano/microbeads, the original porous, large thin film can be converted to a dense, small, thick bulk by a fold-and-press method. The accompanying immunoassay fluorescence signal increases several hundred times. The final immunoassay performance has been demonstrated by direct detection of anti-HSA adsorbed on membranes using HSA-FITC and compared with the original thin electrospun membranes and common NC membranes.

EXPERIMENTAL SECTION

Chemicals. Fluorescein isothiocyanate labeled human serum albumin (HSA-FITC), goat antihuman albumin (anti-HSA), albumin from bovine serum (BSA), poly(caprolactone) (PCL) (MW = 80 kDa), poly(methyl methacrylate) (PMMA) (MW = 120 kDa), sodium azide, and Tween-20 were obtained from Sigma-Aldrich (St. Louis, MO). Nitrocellulose (pore size 0.45 μm) was obtained from Sterlitech (Kent, WA). Amorphous fluoropolymer Teflon AF 2400 1 wt % in FC-75 solvent 400-S1-100-1 was purchased from Dupont (Wilmington, DE). 2,2,2-Trifluoroethanol (TFE, 99.8% purity) purchased from Acros Organics (Geel, Belgium). All of these materials were used as received. Aqueous solutions were prepared with deionized water.

Immunoassay Solutions. Antigen: HSA-FITC, 1 mg/mL stock solution was prepared with phosphate buffer (10 mM phosphate acid, titrated with 1 M NaOH to pH 7.4, and NaN_3 added to 0.02% (w/v)). Antibody: antialbumin antibody produced in goat was diluted to 1 mg/mL with phosphate buffer. Blocking solution: 5% BSA was prepared in phosphate buffer. Rinsing solution: phosphate buffer with 0.2% Tween-20 added.

Electrospinning Method. As illustrated in Figure 1, the electrospinning setup consisted of a Glassman PS/EL30R01.5 high voltage supply, a NE-1000 syringe pump from New Era Pump Systems and a conductive substrate. The electrospinning process and its ambient conditions were monitored using a Motic 2300 USA camera and a Fisher Scientific digital thermometer, respectively. PCL solution prepared by dissolving 1.5 g of PCL into 13.5 g of TFE solvent was continuously fed at 1.5 mL/h

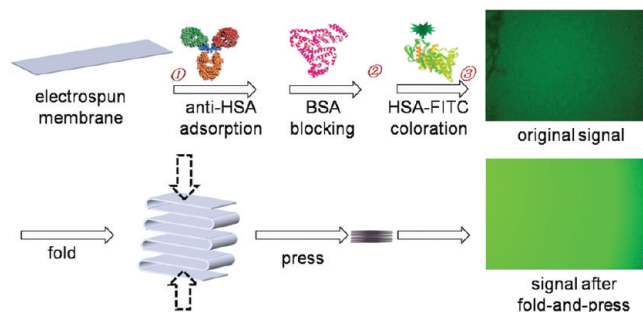


FIGURE 2. Schematic of immunoassay on electrospun membrane with a fold-and-press process. Fluorescence from a 5.3 μm electrospun PCL membrane (25 mm \times 40 mm) after 15 min 1 $\mu\text{g}/\text{mL}$ anti-HSA adsorption, 15 min 5% BSA blocking, 15 min 2 $\mu\text{g}/\text{mL}$ HSA-FITC coloration (top), and from a fold-and-press membrane (bottom).

to the syringe. High voltage of 12 kV was applied between the syringe tip and the collector within a gap of 25 cm. Electrospun PCL fibers were collected on a 5 \times 5 cm^2 metal substrate. The final membrane thickness was controlled by the solution amount dispersed.

Protein Adsorption. Membranes peeled from the Al electrode were cut into 25 mm \times 40 mm coupons, and transferred into HSA-FITC solution of 1 $\mu\text{g}/\text{mL}$ in 10 mM phosphate buffer only or into buffer with 200 mM Na_2SO_4 . The membrane was spread thoroughly by mild shaking for 2 min. The initial fluorescence intensity (A_0) and its change with time (A_t) in the solution were monitored with a NanoDrop 3300 Fluorospectrometer (Thermo Scientific). The percentage of protein adsorbed on membrane was calculated as $(A_0 - A_t)/A_0$.

Signal Enhancement by Fold-and-Press. As shown in the schematic diagram in Figure 2, the membrane was folded and sandwiched between two 1 mm thick rubber layers. Pressure was applied with combination pliers, with a force of ~ 300 N. A fluorescence microscope (Labophot-2, Nikon) coupled with Moticam 5000 cooled CCD camera (Causeway Bay, HK) was used to record the fluorescence intensity from the initial membrane (F_0) and the processed membrane (F_i). This process was repeated several times until no further folding could be accomplished. Final area of $\sim 2 \times 2 \text{ mm}^2$ could be obtained for PCL membranes with initial thickness of 5.3, 11.7, and 24.3 μm . For thicker membranes for 80 and 163 μm , and area of $\sim 4 \times 4 \text{ mm}^2$ was obtained. The fluorescence enhancement from each fold-and-press cycle (g_i) was calculated as F_i/F_{i-1} .

Immunoassay on Membrane. The initial membrane was cut into 25 \times 40 mm^2 pieces and transferred into antibody solution of phosphate buffer with 200 mM Na_2SO_4 . The membrane was spread out in solution by mild shaking for 2 min. The antibody was adsorbed and immobilized by keeping the membrane in solution for 15 min at 25 $^\circ\text{C}$. The membrane was then removed from the solution tube by needle tweezers, and residual solution on the membrane was thoroughly blotted with TechniCloth wipes. The membrane was next transferred into blocking buffer solution, and kept in solution for 15 min at 25 $^\circ\text{C}$. After blocking, the membrane was removed, blotted, and rinsed in PBS buffer for 1 min and blotted dry again. Finally, the membrane was transferred into 2 $\mu\text{g}/\text{mL}$ HSA-FITC solution to complete the antibody–antigen reaction for 15 min at 25 $^\circ\text{C}$. After the immunoassay, the membrane was removed from solution, blotted, rinsed in buffer for 1 min and blotted dry. After several fold-and-press steps to reach the final $\sim 2 \times 2 \text{ mm}^2$ size, the fluorescence was recorded. For the 24.3 μm thick PCL and the commercial nitrocellulose membranes, the same immunoassay procedure was performed except for the fold-and-press process and compared with the folded 5.3 μm PCL membrane.

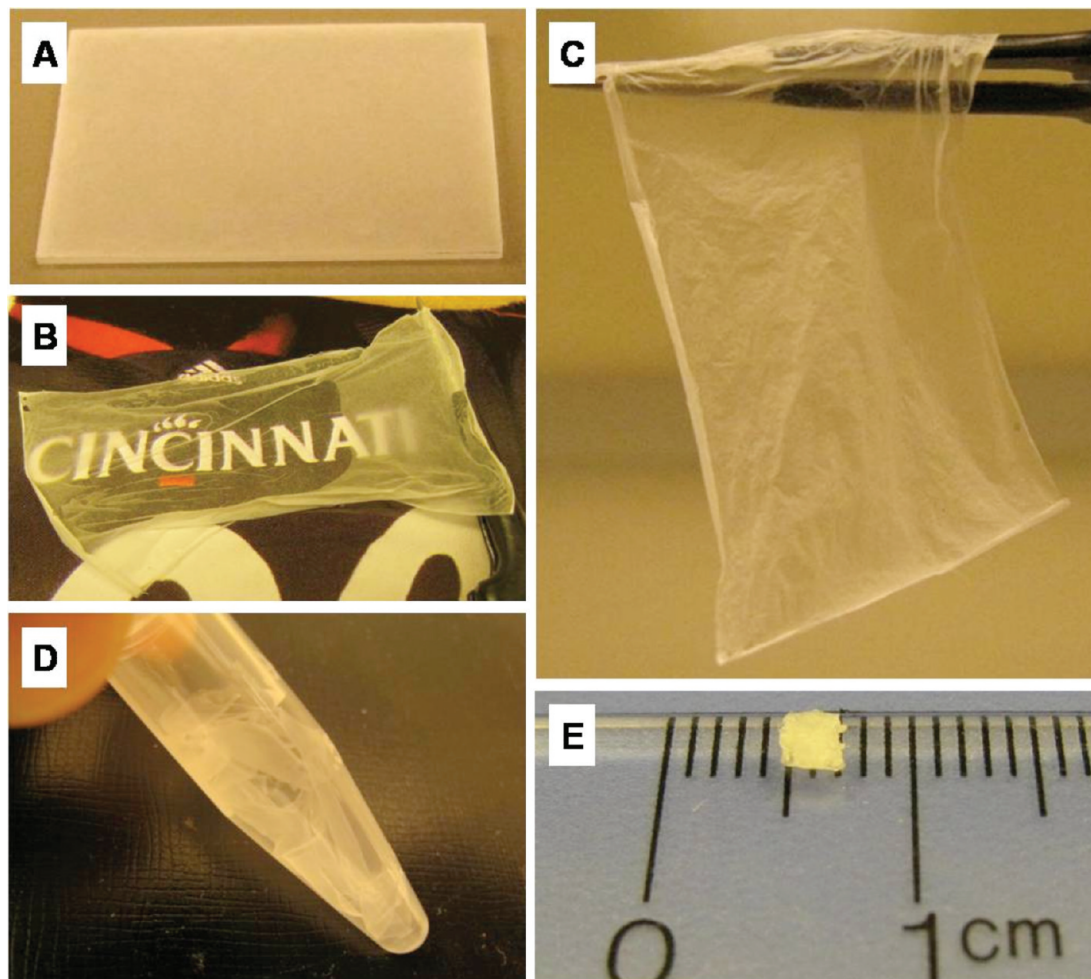


FIGURE 3. Photographs of $5.3 \mu\text{m}$ thick electrospun PCL membrane ($25 \text{ mm} \times 40 \text{ mm}$) on a glass slide surface (A), against color paper (B), free-standing in air (C), dispersed in water (D), and converted to a $2 \times 2 \text{ mm}^2$ dense block after fold-and-press process.

RESULTS AND DISCUSSION

Free-Standing Electrospun PCL Membrane. Surprisingly, the $5.3 \mu\text{m}$ thick PCL membrane can be removed from the substrate electrode easily. It is semitransparent (Figure 3B), free-standing in air (Figure 3C), and displays no self-aggregation. The membrane completely spreads out in solution leading to thorough protein contact and short reaction time on the membrane surface. PCL membranes are stretchable and flexible, and rarely become damaged during manipulation. PCL itself is an FDA-approved implantable biomedical material and widely investigated as a scaffold for drug encapsulation and tissue repair, as it is a polyester from ϵ -caprolactone and degradable in physiological condition. PCL is amorphous at room temperature because of its low glass-transition point (T_g) of $-60 \text{ }^\circ\text{C}$. The tensile strength of electrospun PCL membrane is also very high (3.1 MPa) (11) compared with other membranes. By comparison, the T_g of PMMA is about 120 and $150 \text{ }^\circ\text{C}$ for PC and $50 \text{ }^\circ\text{C}$ for nitrocellulose (depending on the degree of esterification) (19). All these polymers are semicrystalline, stiff, and glassy, and the corresponding electrospun membranes are brittle and cannot be manipulated freely.

The poor mechanical strength of NC in both dry and wet state is an intractable challenge for its conventional applica-

tion, so extreme care and abundant skill are necessary during immunoblotting. NC electrospun membranes from acetone solution can be removed in relatively intact form, but similarly to commercial NC membranes, they are also easily broken when wetted in water. Electrospun PMMA and PC membranes are also very brittle and easily break into powder-like pieces.

The PCL electrospun membrane is not naturally wettable, with a water contact angle (WCA) of $\sim 125^\circ$, although PCL bulk film is moderately wettable (11), with a WCA of $\sim 69^\circ$. Interestingly, when immersed and shaken in water, the $5.3 \mu\text{m}$ thick PCL membrane becomes completely wetted within several minutes (Figure 3D). Much longer time is needed for thicker membranes: $\sim 15 \text{ min}$ for the $11.7 \mu\text{m}$ membrane, and $\sim 1 \text{ h}$ for the $24.3 \mu\text{m}$ membrane. Thicker (80, $163 \mu\text{m}$) membranes cannot be wetted completely, even after 2 days in water.

Two kinds of fibers are found within PCL electrospun membranes. Most are microfibers of $\sim 1\text{--}2 \mu\text{m}$ diameter, and the rest are nanofibers of $\sim 100\text{--}200 \text{ nm}$ diameter (Figure 4A). These fibers are fairly homogeneously distributed within a membrane and do not vary significantly from batch to batch. Due to very high roughness and the re-entrant structure provided by fibers, PCL electrospun mem-

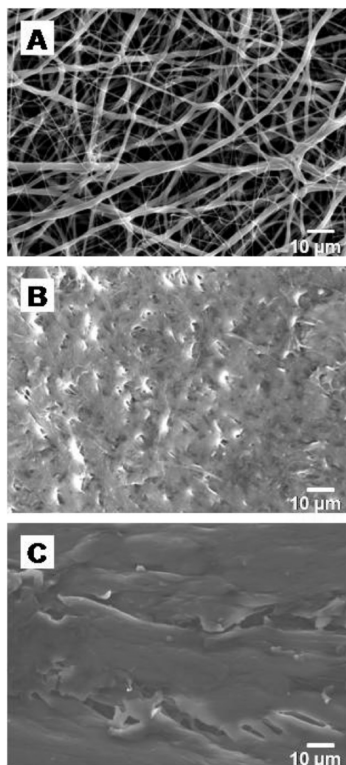


FIGURE 4. SEM micrographs of (A) the initial electrospun PCL membrane surface, (B) the fold-and-press PCL membrane surface, and (C) its cross-section. Before fold-and-press, the PCL membrane (25 mm × 40 mm × 5.3 μm) had been subjected to 1 μg/mL anti-HSA adsorption in 1 mL, 10 mM PBS and 200 mM Na₂SO₄, 5% BSA blocking, 2 μg/mL HSA-FITC reaction, rinsing in 10 mM PBS, and thorough blotting with TechniCloth paper.

branes have a metastable Cassie–Baxter state which provides high WCA. However, under external forces, such as water pressure and shaking, the membrane–water interface can switch to the Wenzel state and become fully wetted (11, 20). Coaxial PCL/Teflon membranes are also mechanically strong enough, but shrink and spontaneously aggregate closely when peeled from the Al electrode because of their superhydrophobic surface, and cannot be spread out in solution.

Protein Adsorption on Electrospun PCL Membrane. When a 40 mm × 25 mm × 5.3 μm PCL membrane was immersed into 1 μg/mL HSA-FITC solution of 10 mM pH 7.4 phosphate, protein was adsorbed on membrane spontaneously and reached the highest amount of 35% (of initial amount in solution as determined by fluorescence measurements) in 40 min, without need of constant shaking (Figure 5A). After this point, the protein adsorption and desorption rates are roughly equal, with no significant additional protein being adsorbed from solution at longer times. Generally, protein can be adsorbed on membranes through several mechanisms, such as hydrophobic, electrostatic, and hydrogen-bond interactions. The PCL electrospun membrane surface in its native state is slightly hydrophobic, and protein can be adsorbed and immobilized on the surface directly via hydrophobic interaction.

The protein adsorption rate and maximum both increased significantly when 200 mM Na₂SO₄ was added into

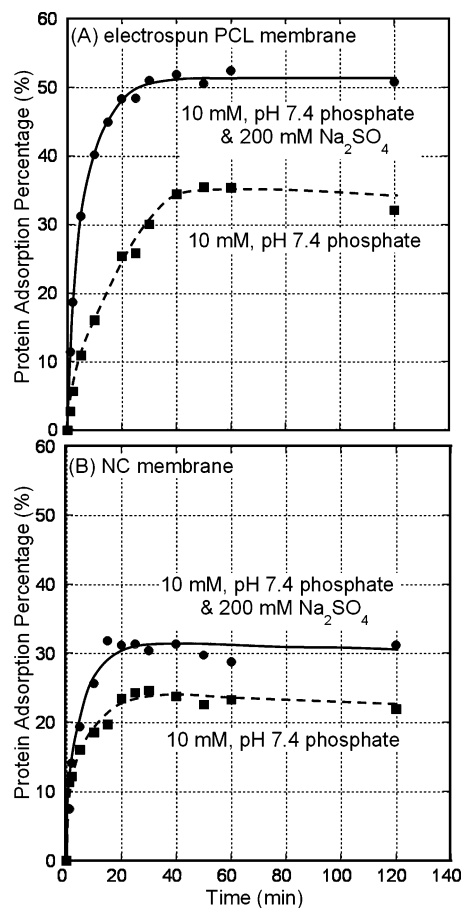


FIGURE 5. Effect of salt addition on protein adsorption on: (A) 1.5 mg electrospun free-standing PCL membrane (40 mm × 25 mm × 5 μm); (B) 1.5 mg commercial nitrocellulose membrane. Membrane was immersed in 1 mL, 1 μg/mL HSA-FITC protein solution, with gentle agitation for nitrocellulose.

the solution (Figure 5A). The addition of the salt increased the protein adsorption maximum amount from 35 to 52%. The adsorption rate prior to saturation (i.e., for short duration) increased from ~1.25%/min to ~2.5%/min. Higher ionic strength is thought to increase the surface hydrophobic interaction between proteins and hydrophobic surface (21).

A NC membrane of the same weight (1.5 mg) as the PCL membrane was also used for protein adsorption test (Figure 5B). In this case, a maximum protein adsorption of ~24% is reached within 20 min without Na₂SO₄, and ~31% in ~15 min with Na₂SO₄. The effect of salt on protein adsorption is not as significant for NC membranes, because most protein is adsorbed on the surface via mixed electrostatic and hydrophobic interactions (22).

The protein adsorption per unit area of the membrane can be calculated. From the SEM photograph (Figure 4A) of the PCL membrane, the fiber diameter (d) is estimated to have an average value of ~1 μm. The weight (w) of this PCL membrane is 1.5 mg and the density (ρ) of PCL is 1.145 g/cm³. The total surface area (S) of PCL fiber in the membrane can be calculated as $S = 4w/(d\rho)$, equal to ~52 cm². For 52% maximum adsorption of the initial protein amount (Figure 5A), the protein density on fiber surface is ~10 ng/cm². The maximum protein density that can be obtained on a single-layer surface is ~200 ng/cm² (23).

Several factors can affect the adsorbed protein amount. First are the properties of the protein molecule itself and its FITC tags. Approximately 10 FITC molecules are attached to one HSA molecule (Sigma product information), making this protein more negatively charged than the original positive (or neutral) amino groups, and changing the molecule size and shape. Second, tiny air bubbles can be trapped into PCL fibers. These reduce the effective surface area available for protein adsorption. The third factor has to do with the kinetics of protein adsorption. The equilibrium constant (K) of HSA-FITC on electrospun PCL membrane is given by

$$K = \frac{P_{\text{bond}}}{P_{\text{free}}C_{\text{free}}} = \frac{P_{\text{bond}}}{(P_{\text{max}} - P_{\text{bond}})C_{\text{free}}}$$

where P_{bond} is the density of surface sites bonded with protein (10 ng/cm²), P_{max} is the density of maximum available surface sites (200 ng/cm²), P_{free} is the density of free surface locations (190 ng/cm²), and C_{free} is the free protein concentration in solution. For the initial protein concentration of 15 nM of which 52% is adsorbed on the membrane, C_{free} is about 7.5 nM. K is then calculated to be $\sim 7 \times 10^6 \text{ M}^{-1}$. This binding constant between electrospun PCL membrane and HSA-FITC is consistent with other binding constants of proteins on hydrophobic surfaces (24). This confirms that electrospun PCL membranes surface are suitable for antibody immobilization via direct hydrophobic adsorption.

Covalent antibody immobilization methods on electrospinning membranes have also been reported. This includes click chemistry of azidized-antibody to electrospun membrane of propargyl-containing polymer for immunoassay of testis-specific protease (25), electrospinning of carboxyl or amino functional polymers for chemical derivation to antibody coupling (18), and molecular imprinting to generate molecule recognition sites on electrospun fibers for 2,4-dichlorophenoxyacetic acid detection (26). Compared with these previously reported covalent methods, the direct protein adsorption presented here is much faster and simpler with acceptable efficiency.

Signal Amplification by Fold-and-Press Process. The effective fluorescence signal from a single layer thin electrospun PCL membrane is relatively limited (Figure 6). The high porosity ($\sim 75\%$) and low thickness (5.3 μm) of the PCL membrane are specific advantages for easy protein immobilization and fast immunoreactions. However, these characteristics also result in a much lower signal from a single layer membrane than that from common NC membranes. To overcome this obstacle, a fold-and-press process is added after immunoassay to effectively “concentrate” the signal, in which all signal molecules distributed across the membrane are collected into a very small volume for easy detection by conventional fluorescence microscopy.

Signals from electrospun membranes with and without fold-and-press process were compared. After folding and pressing 8 times for the thin membranes (5.3, 11.7, and 24.3 μm), bulk-like samples of approximately $2 \times 2 \text{ mm}^2$ were obtained (Figure 3E). The thicker membranes (80, 163 μm) underwent 6 fold-and-process cycles, resulting in $\sim 4 \times 4 \text{ mm}^2$ size. The fluorescence signal of native PCL membranes

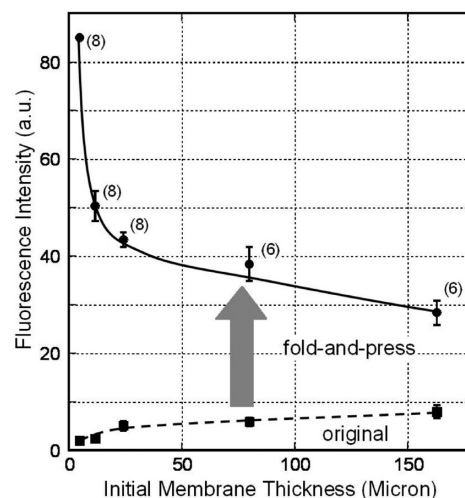


FIGURE 6. Effect of electrospun PCL membrane thickness on fluorescence intensity for single layer membranes and for fold-and-press samples after immunoassay with 1 $\mu\text{g}/\text{mL}$ anti-HSA. Number of fold-and-press cycles is in parentheses.

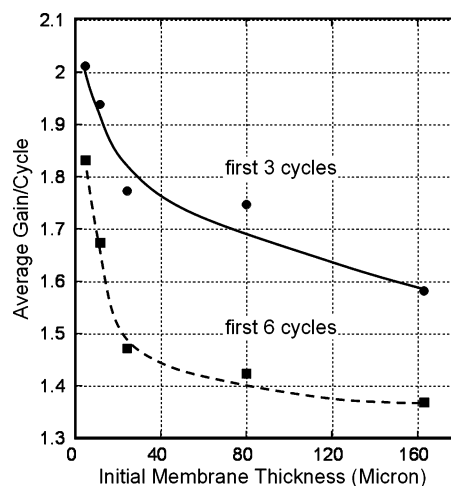


FIGURE 7. Average gain per cycle of fluorescence intensity with membrane thickness after immunoassay with 1 $\mu\text{g}/\text{mL}$ anti-HSA.

increased with thickness, from ~ 1.9 at 5.3 μm to ~ 7.9 at 163 μm (Figure 6). For fold-and-press PCL samples, the final fluorescence signal decreased with increasing initial membrane thickness, from 85 (saturation) at 5.3 μm to 18 ± 2.5 at 163 μm . The signal gain (g) provided by the fold-and-press process is shown in Figure 7. For the first 3 folding cycles, the average gain was 2.01 for the 5.3 μm membrane, but only 1.58 for the 163 μm membrane. For the first 6 cycles, the average gain was 1.83 and 1.36 for the 5.3 and 163 μm membranes, respectively. The gain/cycle decreased gradually with the number of cycles, which can be attributed to fluorescent signal reabsorption and scattering through the increasing sample thickness. The final sample thickness was $\sim 280 \mu\text{m}$ for the initial 5.3 μm membrane, and $\sim 650 \mu\text{m}$ for the 11.7 μm membrane after 8 cycles (Table 1). Therefore, only 5.3 μm membranes were utilized in the following immunoassay experiments.

To determine the optimal fold-and-press process sequence, immunoassay signals obtained from samples with fold-and-press at different points are compared in Table 2. For anti-HSA concentration ranging from 100 ng/mL to 10

Table 1. Electrospun PCL Membrane Thickness^a

liq (μL)	50	100	200	500	1000
t_a (μm)	5.3	11.7	24.3	80	163
t_b (μm)	280	650	1410	N/A	N/A

^a liq, polymer solution dispersed for electrospinning; t_a , membrane thickness as electrospun; t_b , sample thickness after 8 cycles of fold-and-press.

Table 2. Immunoassay Fluorescence Intensity from Electrospun PCL Membranes with Fold-and-Press at Different Points in the Process^a

anti-HSA conc	before anti-HSA adsorption (1)	before HSA-FITC reaction (2)	after HSA-FITC reaction (3)
10 $\mu\text{g/mL}$	16 \pm 0.44	67 \pm 11	85 (sat)
1 $\mu\text{g/mL}$	7.7 \pm 0.21	33 \pm 4.2	85 (sat)
100 ng/mL	4.1 \pm 0.1	20 \pm 1.5	75 \pm 5.6

^a ①, ②, ③: see labels in Figure 2; sat: saturated signal.

$\mu\text{g/mL}$, it was found that performing the fold-and-press after immunoassay can most effectively amplify the signal with all three anti-HSA concentrations. Fold-and-press prior to anti-HSA immobilization was the least effective sequence. For a 1 $\mu\text{g/mL}$ anti-HSA concentration, this results in a signal of 7.7 \pm 0.2, similar to the immunoassay signal from a single initial 24.3 μm membrane. It is proposed that anti-HSA molecules cannot access the fiber surface within the folded membrane, resulting in limited antibody immobilization and subsequent HSA-FITC/anti-HSA reaction. It is important to point out that using an electrospun PC membrane that was simply densified by pressure resulted (15) in a much smaller improvement in immunoassay signal than what is presented here. Protein immobilization on nanoporous PC film is intrinsically inefficient, as only a single-layer surface with some nanopores embedded can be utilized. If the membrane is folded and pressed after anti-HSA but before HSA-FITC immunoreactions, the immunoassay signal is a little higher (33 \pm 4.2). In this case, the HSA-FITC probably could not make contact with the anti-HSA molecules hidden inside the membrane, although large amount of antibody molecules have been immobilized on and within the membrane.

The signal gain after n cycles is calculated as g^n , where g is the average gain/cycle. For the initial 5.3 μm membrane, g is 1.83/cycle averaged over 6 cycles. After 6 cycles, this resulted in a total final gain of \sim 38. For the ideal gain/cycle of 2, the total gain after 6 cycles will be 64. Therefore, at this point, slightly more than half of the ideal signal increase has been obtained. Significantly, another factor of \sim 2 increase is potentially achievable.

The gain provided by the fold-and-press process is similar to DNA amplification with polymerase chain reaction (PCR). In PCR, the gain per cycle is \sim 1.5. After 30–40 cycles, PCR results in a signal increase of several million times. In the free-standing electrospun membrane immunoassay system, currently a maximum of 8 folding cycles can be applied to the thinnest (5.3 μm) membranes. To maximize signal amplification, we need to develop much thinner membranes. In recent years, polymer or composite membranes of \sim 30 nm thickness have been reported by spin coating or solution filtering (27, 28).

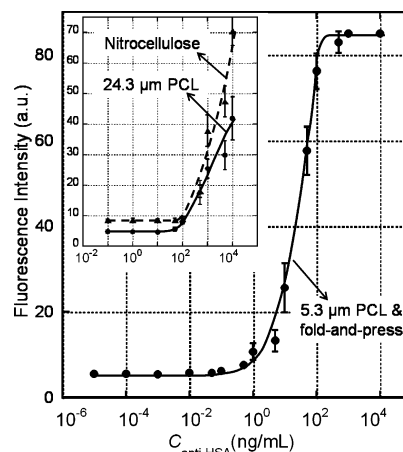


FIGURE 8. Immunoassay fluorescence intensity on 5.3 μm electrospun PCL membrane ($25 \times 40 \text{ mm}^2$) after fold-and-press, 24.3 μm electrospun PCL membrane ($2 \times 4 \text{ mm}^2$), and nitrocellulose membrane ($2 \times 4 \text{ mm}^2$).

If a final folded membrane sample of 300 μm can be obtained from an initial membrane of 30 nm, this would consist of 13–14 folding cycles. For an ideal gain per cycle of 2, this would result in a final signal gain of \sim 10 000.

Sensitive Immunoassay on Electrospun Membranes. To determine the limit of detection (LOD) and linear range of immunoassay on the PCL membranes, anti-HSA was adsorbed directly on a 40 mm \times 25 mm \times 5.3 μm PCL membrane, a 2 mm \times 4 mm \times 24.3 μm PCL membrane, and a 2 mm \times 4 mm \times 150 μm nitrocellulose membrane for comparison. The samples were then blocked with 5% BSA, and finally reacted with 2 $\mu\text{g/mL}$ HSA-FITC. After the 5.3 μm PCL membrane was converted into a 2 mm \times 2 mm sample by the fold-and-press process, the fluorescence was recorded for all samples.

On the 5.3 μm fold-and-press PCL membrane, immunoassay tests were performed from 10 $\mu\text{g/mL}$ to 10 fg/mL (Figure 8). The linear detection range was determined from 500 ng/mL to 1 ng/mL with an r^2 (correlation coefficient) of 0.96. The LOD was 0.080 ng/mL with the blank control fluorescent intensity of 5.5 \pm 0.2. The corresponding molar concentration was \sim 560 fM. This sensitivity is higher than those from most direct fluorescence immunoassays on membranes and protein chips. On the single layer 24.3 μm PCL membranes, the blank control and LOD were 4.8 \pm 0.5 and 74 ng/mL, respectively. For the NC membrane, the values were 8.5 \pm 0.3 and 120 ng/mL. Both of these membranes had a linear detection ranging from 50 ng/mL to 10 $\mu\text{g/mL}$ (Figure 8). This is well in accord with common immunoassay sensitivity (4). Using 1 $\mu\text{g/mL}$ phosphorylase B, negative controls were also measured as 5.3 \pm 0.2 on 5.3 μm fold-and-press PCL membrane, 4.7 \pm 0.4 on 24.3 μm PCL membrane, and 8.6 \pm 0.6 on NC. The results for the negative controls were very similar to the blank control levels. This indicates that no crossover reaction occurred between the negative control protein and the coloration protein.

By comparison, PC electrospun membrane immunoassay within a microfluidic device has an IgG LOD of \sim 1 $\mu\text{g/mL}$, because only a single layer surface could be utilized in that

case (15). On carboxyl functional PVC electrospun membranes, 1–100 ng/mL SEB could be detected from enzyme-amplified chemiluminescent signal (18). Using the chemiluminescence detection method for human fibronectin blotting, similar detection limits (20 ng/mL) were obtained on commercial nitrocellulose, nylon membranes and their corresponding electrospun membranes (17). Although the approximately femtomolar to attomolar limit has been reached by immune-PCR and biobarcode assay (BCA), the preparation of functional nanobeads requires significant efforts, and the signal amplification by PCR takes significant additional time (6).

In the results reported here, the total time for completing the immunoassay was ~50 min with anti-HSA and HSA-FITC on free-standing electrospun PCL membrane. In the future, it should be possible to complete the entire immunoassay process within 10 min. This will require that the capture antibody immobilization and surface blocking be carried out on the electrospun membrane in advance, and the immunoreaction between detection antibody and antigen to take place homogeneously in one step in solution, instead of multistep heterogeneously on the membrane/solution interface (29), and be followed by fast collection by capture antibody on membrane.

CONCLUSION AND OUTLOOK

The thin free-standing electrospun membranes as bioassay substrates possess two specific advantages over conventional membranes and nano/microbeads. First, nano/micro continuous fibers can be easily and cheaply fabricated by electrospinning from a variety of bio/polymer materials. The resulting very large surface area (50 cm²/1.5 mg) can be easily accessed similarly to that obtainable with nanobeads, and surface related immunoassay can be completed within short times. Using continuous membranes, collection, and redispersing are straightforward and take much shorter time (<10 s) than on NC membranes or when using nanobeads. Second, electrospun membranes have micropores with large diameter (>1 μm) and shallow depth (<6 μm). Large biomolecules can access freely the inner surface of the electrospun membrane, resulting in faster antibody immobilization and subsequent immunoreactions, and easy nonspecific protein rinsing and lower background signals.

More specifically, PCL electrospun membranes display greater tenacity than most other common polymers due to the lower T_g . The membrane can be handled freely, even if it is only a few micrometers thick. It can be readily removed from substrates, be freestanding in air, picked directly by tweezers from solution, blotted instantly by filter paper, and dispersed fast into other buffers. After immunoassay, the polymer can be folded and pressed from the starting porous thin membrane into a dense bulklike thick film, leading to significant signal amplification (>120 ×). Finally, PCL has the appropriate surface energy, so the thin membrane can be extended easily in solution, and protein molecules can be adsorbed and immobilized effectively by hydrophobic interaction.

Future increases in immunoassay sensitivity on free-standing membrane are possible with some straightforward

improvements in the materials and process utilized. First, decreasing the electrospun fiber diameter directly increases surface area. More antibodies immobilized on the surface area will lead to more antigen binding and higher signal. Second, using coaxial electrospinning, many well-known ultralow adsorption polymers, such as gelatin and functionalized PEO, can be coaxially electrospun as needed for fiber sheath with PCL as core material to retain whole membrane tenacity. The sheath can be modified for antibody immobilization and nonspecific protein adsorption resistance, which will lead to lower background. Finally, with these sheath materials, the surface will be more hydrophilic, so the membrane can be wetted faster, and trapping of air bubble can be inhibited.

REFERENCES AND NOTES

- Thomas, P. S. *Proc. Natl. Acad. Sci. U.S.A.* **1980**, *77*, 5201–5205.
- Burnette, W. N. *Anal. Biochem.* **1981**, *112*, 195–203.
- Deblas, A. L.; Cherwinski, H. M. *Anal. Biochem.* **1983**, *133*, 214–219.
- Morgan, C. L.; Newman, D. J.; Price, C. P. *Clin. Chem.* **1996**, *42*, 193–209.
- Michalet, X.; Pinaud, F. F.; Bentolila, L. A.; Tsay, J. M.; Doose, S.; Li, J. J.; Sundaresan, G.; Wu, A. M.; Gambhir, S. S.; Weiss, S. *Science* **2005**, *307*, 538–544.
- Nam, J. M.; Thaxton, C. S.; Mirkin, C. A. *Science* **2003**, *301*, 1884–1886.
- Sano, T.; Smith, C. L.; Cantor, C. R. *Science* **1992**, *258*, 120–122.
- Chen, Z.; Tabakman, S. M.; Goodwin, A. P.; Kattah, M. G.; Darancioglu, D.; Wang, X. R.; Zhang, G. Y.; Li, X. L.; Liu, Z.; Utz, P. J.; Jiang, K. L.; Fan, S. S.; Dai, H. J. *Nat. Biotechnol.* **2008**, *26*, 1285–1292.
- Li, D.; Xia, Y. N. *Adv. Mater.* **2004**, *16*, 1151–1170.
- Yoshimoto, H.; Shin, Y. M.; Terai, H.; Vacanti, J. P. *Biomaterials* **2003**, *24*, 2077–2082.
- Han, D. W.; Steckl, A. J. *Langmuir* **2009**, *25*, 9454–9462.
- Choi, S. W.; Jo, S. M.; Lee, W. S.; Kim, Y. R. *Adv. Mater.* **2003**, *15*, 2027–2032.
- Wang, X. Y.; Drew, C.; Lee, S. H.; Senecal, K. J.; Kumar, J.; Sarnuelson, L. A. *Nano Lett.* **2002**, *2*, 1273–1275.
- Liu, H. Q.; Kameoka, J.; Czaplowski, D. A.; Craighead, H. G. *Nano Lett.* **2004**, *4*, 671–675.
- Yang, D. Y.; Niu, X.; Liu, Y. Y.; Wang, Y.; Gu, X.; Song, L. S.; Zhao, R.; Ma, L. Y.; Shao, Y. M.; Jiang, X. Y. *Adv. Mater.* **2008**, *20*, 4770–4775.
- Wu, D. P.; Steckl, A. J. *Lab Chip* **2009**, *9*, 1890–1896.
- Manis, A. E.; Bowman, J. R.; Bowlin, G. L.; Simpson, D. G. *J. Biol. Eng.* **2007**, *1*:2, doi:10.1186/1754-1611-1-2.
- Senecal, A.; Magnone, J.; Marek, P.; Senecal, K. *React. Funct. Polym.* **2008**, *68*, 1429–1434.
- Lide, D. R. *Handbook of Chemistry and Physics*, 78th ed.; CRC Press: Boca Raton, FL, 1998; p 13(4–11).
- Lafuma, A.; Quere, D. *Nat. Mater.* **2003**, *2*, 457–460.
- Chen, J.; Sun, Y. *J. Chromatogr., A* **2003**, *992*, 29–40.
- Farrah, S. R.; Shah, D. O.; Ingram, L. O. *Proc. Natl. Acad. Sci. U.S.A.* **1981**, *78*, 1229–1232.
- Sigal, G. B.; Mrksich, M.; Whitesides, G. M. *J. Am. Chem. Soc.* **1998**, *120*, 3464–3473.
- Zhang, J.; Kinsel, G. R. *Langmuir* **2003**, *19*, 3531–3534.
- Shi, Q.; Chen, X. S.; Lu, T. C.; Jing, X. B. *Biomaterials* **2008**, *29*, 1118–1126.
- Chronakis, I. S.; Milosevic, B.; Frenot, A.; Ye, L. *Macromolecules* **2006**, *39*, 357–361.
- Vendamme, R.; Onoue, S. Y.; Nakao, A.; Kunitake, T. *Nat. Mater.* **2006**, *5*, 494–501.
- Endo, H.; Mitsuishi, M.; Miyashita, T. *J. Mater. Chem.* **2008**, *18*, 1302–1308.
- Georganopoulou, D. G.; Chang, L.; Nam, J. M.; Thaxton, C. S.; Mufson, E. J.; Klein, W. L.; Mirkin, C. A. *Proc. Natl. Acad. Sci. U.S.A.* **2005**, *102*, 2273–2276.

AM900664V